Pergamon

PII: S0191-8141(97)00023-0

Journal of Structural Geology, Vol. 19, No. 7, pp. 909 to 925, 1997

0191-8141/97 $17.00 + 0.00

Texture development in experimentally deformed two-phase aggregates of calcite and anhydrite

DAVID F. BRUHN* and MARTIN CASEY†

Geologisches Institut, ETH Zürich, CH-8092 Zürich, Switzerland

(*Received* 11 *March* 1996; *accepted in revised form* 31 *January* 1997)

Abstract—Fully quantitative textures have been measured from experimentally deformed two-phase aggregates of calcite and anhydrite. Two sets of deformation experiments were performed. Firstly, to investigate the development of microstructure and texture with composition, samples with varying volume proportions of calcite and anhydrite were deformed to 20% strain at identical conditions. Secondly, to study the texture development of the two materials with strain and explore the possible use of texture index as a strain gauge in polyphase materials, pure calcite and pure anhydrite were deformed at the same conditions as the two-phase rocks to strains of 6%, 12% and 20%.

The textures in both calcite and anhydrite were found to be similar, but not identical, to those reported in previous studies for pure samples. Our experimental investigations and measured textures show that the textures both of the pure materials and of the two-phase rocks depend not only on strain but also on stress and grain size, through their influence on the deformation mechanisms. The dependence of texture index with change in deformation mechanism is particularly pronounced in the anhydrite component, where the texture index decreases with grain size, which decreases with anhydrite content. The texture in the pure calcite and in the calcite component of the two-phase rocks was influenced by a preexisting fabric. The intensity of the texture in the deformed samples seems to correlate with the stress in the calcite rather than with strain. © 1997 Elsevier Science Ltd.

INTRODUCTION

The development of a crystallographic preferred orientation (CPO) in a polycrystalline aggregate during deformation depends critically on stress and/or strain rate, temperature, pressure and strain (e.g. Tullis *et al.*, 1973; Wenk *et al.*, 1973; Kern, 1977). For materials deformed at identical temperature/strain rate conditions, model calculations predict that textures strengthen with strain (e.g. Lister and Hobbs, 1980). A positive correlation of strain with fabric intensity has been shown for both naturally (e.g. Marjoribanks, 1976; Bouchez, 1977; Law *et al.*, 1984) and experimentally (e.g. Tullis *et al.*, 1973; Casey *et al.*, 1978; Dell'Angelo and Tullis, 1986) deformed rocks. Thus, it seems that that texture might be used to at least approximately determine the relative amount of strain in a material. Similarly, the intensity of the CPO of a mineral phase within a polyphase aggregate may potentially be used to determine the strain of that mineral provided that its CPO development has been calibrated with strain in a single phase. However, the development of a CPO in a mineral within a polyphase aggregate may differ from that in a monomineralic aggregate. As the crystallographic preferred orientations of a mineral depend on the active slip systems in the crystals, there are several possibilities of how the presence of another phase might influence the development of the texture: (a) slip systems that are active in a single phase material at equivalent conditions may be inhibited by another phase due to grain boundary constraints; (b) grain boundary sliding at the interphase boundaries might contribute significantly to the overall strain, reducing the amount of intracrystalline deformation and consequently the intensity of the texture; and (c) differences in strength between the phases may lead to a localization of the strain into the weaker phase, leading to only a weakly developed texture in the stronger phase. Generally, (a) and (b) need to be addressed first if CPO intensity is to be used to investigate point (c).

In this study, we seek to investigate the extent to which the assumption that the CPO of a mineral within a polyphase rock may be used to provide a measurement of that mineral's strain is true. For this investigation, we compared the evolution of CPO in experimentally deformed synthetic single-phase aggregates of calcite and anhydrite with that observed in synthetic two-phase aggregates of calcite and anhydrite deformed at the same conditions.

Previous work and scientific approach

Several studies on CPO development in both naturally and experimentally deformed polyphase rocks (e.g. Starkey and Cutforth, 1977; Kronenberg, 1981; Lisle, 1985; Dell'Angelo and Tullis, 1986; Jordan, 1987; Tullis and Wenk, 1994) seem to give somewhat contradictory results. In a study on the quartz c-axis preferred orientations in naturally deformed rock samples with varying quartz content from two different localities, Starkey and Cutforth (1977) found a linear correlation

*Present address: Department of Geology and Geophysics, University of Minnesota, Minneapolis, MN 55455, U.S.A.

†Present address: Department of Earth Sciences, The University, Leeds LS2 9JT, U.K.

between the amount of quartz present and the intensity of preferred orientation. However, no information was given on the amount of strain in the rocks or in the quartz component. A similar observation to that of Starkey and Cutforth (1977) was reported by Lisle (1985) in a study on the c-axis preferred orientation of quartz in pebbles from a naturally deformed conglomerate. The strength of the CPO seems to be correlated to the quartz content of the pebbles, rather than to the strain in the pebbles; but again, no information was given on the amount of finite strain in the quartz. Kronenberg (1981) investigated the variation of quartz c-axis preferred orientation in pebbles with varying quartz and mica contents from a naturally deformed conglomerate. The CPO was found to be very strongly developed in pure quartzites, but random in fine-grained quartz–mica layers, where the mica developed a strong CPO. From these observations, Kronenberg (1981) concluded that the presence of mica allowed enhanced grain boundary sliding and quartz grain rotation without internal deformation of the quartz. In experimentally deformed synthetic quartz–muscovite rocks, Tullis and Wenk (1994) observed that pure quartz developed a stronger c-axis preferred orientation at 35% and 50% strain than quartz samples with the addition of 25% and 50% muscovite. Moreover, while the intensity of the quartz texture in samples with 25% muscovite increased with strain, textures in samples containing 50% muscovite were similar at 35% and 50% strain. Dell'Angelo and Tullis (1986) investigated the quartz c-axis preferred orientations in experimentally deformed aplites containing 30% quartz, and compared them with those in pure quartzites. No change in pattern and strength of the CPO with composition was found. The CPO was observed to become stronger with increasing strain in the quartz component. The intensity of the CPO for a given strain and the quartz grain strains were similar in both pure quartzite and aplite, suggesting that the presence of feldspar has no significant effect on the operative slip systems in quartz at the deformation conditions. In synthetic calcite–halite samples deformed by Jordan (1987), pure calcite was deformed by cataclastic flow and twinning, whereas halite was deformed by dislocation creep. Jordan (1987) found that the intensity of the CPO of calcite c-axes increased with strain, but that with increasing halite content, the intensity of calcite CPO decreased and changed only slightly with increasing strain.

However, most of these studies are not very well constrained. In particular, they have concentrated on rocks containing two or more phases of high strength contrast, thereby complicating the separation of the effect on the CPO evolution of the second phases inducing different deformation mechanisms from the effect of strain partitioning between the phases. In some of the studies (Jordan, 1987; Tullis and Wenk, 1994), the decreasing intensity of the CPO with increasing amount of second phase was explained by strain partitioning into

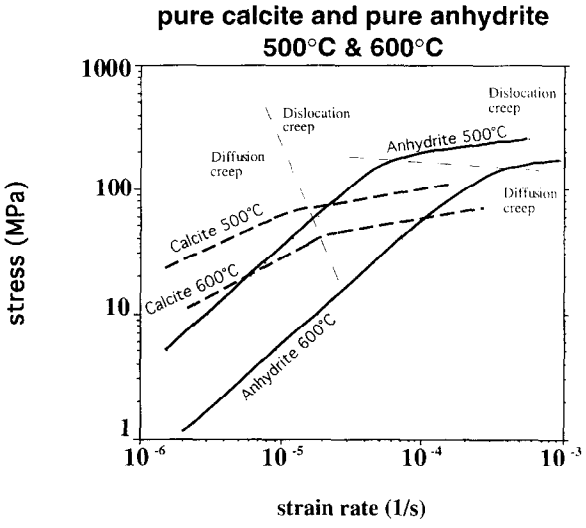

Fig. 1. The flow stress of synthetic fine-grained aggregates of calcite (Olgaard and Dell'Angelo, 1993) and anhydrite (Dell'Angelo and Olgaard, 1995) at 500°C and 600°C as a function of strain rate.

the weaker phase, in others by enhanced grain boundary sliding along interphase boundaries (Starkey and Cutforth, 1977; Kronenberg, 1981; Lisle, 1985), reducing the contribution of intracrystalline deformation to the sample strain. In the aplite studied by Dell'Angelo and Tullis (1986), quartz was the weaker phase, and it accommodated a considerable amount of strain and developed a strong CPO, equal to that observed for pure quartzite. The correlation of strain and strength of preferred orientation in the quartz component, independent of the presence of feldspar, is emphasized by Dell'Angelo and Tullis (1986), although they pointed out that the intensities of the CPO in quartz should increase rather than decrease with increasing (rigid) feldspar content, because quartz would have to undergo more strain to accomplish the same sample strain.

Hoping to avoid some of the problems arising from the analysis of materials with phases of high competence contrast, we have undertaken an experimental study to investigate the deformation behaviour and the texture development in a fine-grained two-phase rock, containing two phases of similar strengths. Of the potential minerals satisfying this requirement, calcite and anhydrite were chosen as the end-member phases because the mechanical properties of synthetic fine-grained aggregates of each have been well-characterized in previous studies (calcite: e.g. Walker *et al.*, 1990; Olgaard and Dell'Angelo, 1993; anhydrite: e.g. Dell'Angelo and Olgaard, 1995). Moreover, the evolution of the CPO of these minerals during deformation is well established (calcite: e.g. Wenk *et al.*, 1973, 1981; Casey *et al.*, 1978, 1991; Spiers, 1979; Wenk, 1985; Rutter *et al.*, 1994; anhydrite: e.g. Müller *et al.*, 1981; Mainprice *et al.*, 1993; Dell'Angelo and Olgaard, 1995). At the chosen experimental conditions, the strength contrast between the two pure end-members is less than 2 (Fig. 1), and thus it is not obvious from optical microstructures alone as to how the

presence of each phase influences the CPO of either calcite or anhydrite.

The goals of this study are: (a) to evaluate how the intensities of the textures change with strain in pure calcite and pure anhydrite samples deformed at similar conditions; (b) to investigate the textural development in the two-phase rocks with varying volume proportions of each phase, when deformed at identical conditions; and (c) to determine whether the intensities of the textures can be used to estimate the amount of strain in a phase within the two-phase rocks. This is the first time that a fully-quantitative examination of texture development of both phases in a two-phase rock has been reported in the earth science literature.

DEFORMATION EXPERIMENTS

Starting materials

The starting materials for the fabrication of the samples used in this study were reagent grade powders of hemihydrate ($CaSO_4 \cdot 1/2H_2O$) and calcite ($CaCO_3$) with a purity >99%. These were the same powders as used for the anhydrite experiments of Dell'Angelo and Olgaard (1995) and the calcite experiments of Olgaard and Dell'Angelo (1993). After the fabrication procedures described below, the mean grain size of the anhydrite rocks was 8 μm, and that of the calcite rocks was 7–10 μm. For the calcite/anhydrite mixtures, the final average grain sizes vary between 2 and 3 μm for either phase, depending on composition (Table 1).

Sample preparation

The synthetic rocks used in the experiments were made in three steps: (1) mixing of the powders, (2) uniaxial cold-pressing of the powder mixtures, and (3) hot isostatic pressing (HIPing). For the production of the two-phase rocks, the calcite and anhydrite–hemihydrate powders were mixed in volume proportions of 90:10, 70:30, 50:50, 30:70, and 10:90 calcite:anhydrite (Cc:An). Two batches of the 50:50 mixture were made. The first one, referred to as 50:50 HIP#1, was mixed as a suspension in ethanol by rolling in a closed plastic container for ~24 h. However, there was a tendency for the anhydrites to form clusters of 10–20 grains (e.g. Figure 2a). To avoid these clusters, large alumina balls (diameter approx. 2 cm) were added to the ethanol–powder suspension, and then the containers were rolled for 24 h. The 50:50 mixture made by this method is referred to here as 50:50 HIP#2. All the other mixtures were mixed using the alumina balls.

After mixing, the powders were dried on a hot-plate, sieved to remove the alumina balls, and then cold-pressed uniaxially with a hydraulic press at an applied load of 50 tons. Then, the powders were hot-isostatically pressed (HIPed) at 550°C and a confining pressure of 200 MPa for 4 h. The final porosity of the resulting rocks was generally <4%. From these rocks, samples were cored for the deformation experiments and/or texture goniometry.

Experimental conditions

All the deformation experiments were performed in axial compression in a gas confining deformation apparatus at 500°C, at a constant deformation rate, corresponding to a strain rate of $5 \times 10^{-5}\,s^{-1}$ and a confining pressure of 300 ± 10 Mpa. Samples were jacketed in copper tubes. The final stress values have been corrected for the strength of the copper jackets. Two sets of experiments were performed: (a) samples of all the different mixtures were deformed to 20% strain; and (b) samples of the two pure end-member materials were deformed to strains of 6%, 12% and 20%. The term 'strain', as used for the experimentally deformed aggregates of this study, is always the 'true' logarithmic strain.

Under these experimental conditions, deformation of the calcite made from reagent grade powders is dominantly by dislocation creep (Olgaard and Dell'Angelo, 1993), and most of the sample strain is accommodated by grain flattening.

Table 1. Grain sizes and grain aspect ratios for calcite/anhydrite aggregates

Experiment no.	Mixture Cc:An (vol.%)	No. of grains (parallel)		No. of grains (perpendicular)		Grain size (μm) (parallel)		Grain size (μm) (perpendicular)		Grain flattening (%)		
		Cc	An	Cc	An	Cc	An	Cc	An	Cc	An	Total
*H1185	90:10	441	92	342	87	3.4	1.8	4.5	2.0	17.0	7.0	8.9
H1199	90:10	318	35	244	35	2.7	2.7	3.6	2.8	19.1	4.7	17.6
		297	41	233	35	2.8	2.2	3.9	2.8	18.1	14.5	17.7
H1215	70:30	235	132	203	109	2.8	2.1	3.4	2.8	13.3	15.2	13.9
	70:30	258	128	199	105	2.6	2.2	3.6	2.8	18.5	16.2	17.8
H1202	30:70	146	263	131	232	2.0	2.6	2.1	3.0	10.1	10.7	10.5
		152	268	125	230	1.9	2.4	2.4	3.0	15.4	13.5	14.0
H1203	10:90	173	554	119	411	2.0	3.6	3.0	4.8	22.0	18.2	18.8
H1150	50:50#1	276	245	237	220	2.7	2.3	3.2	2.6	10.9	8.2	9.7
*H1185	50:50#1	216	232	187	200	3.2	4.1	3.9	4.9	10.8	11.1	11.0
H1198	50:50#2	182	184	151	142	2.7	2.7	3.2	3.5	11.4	17.1	14.3

*Undeformed, annealed at 600°C.

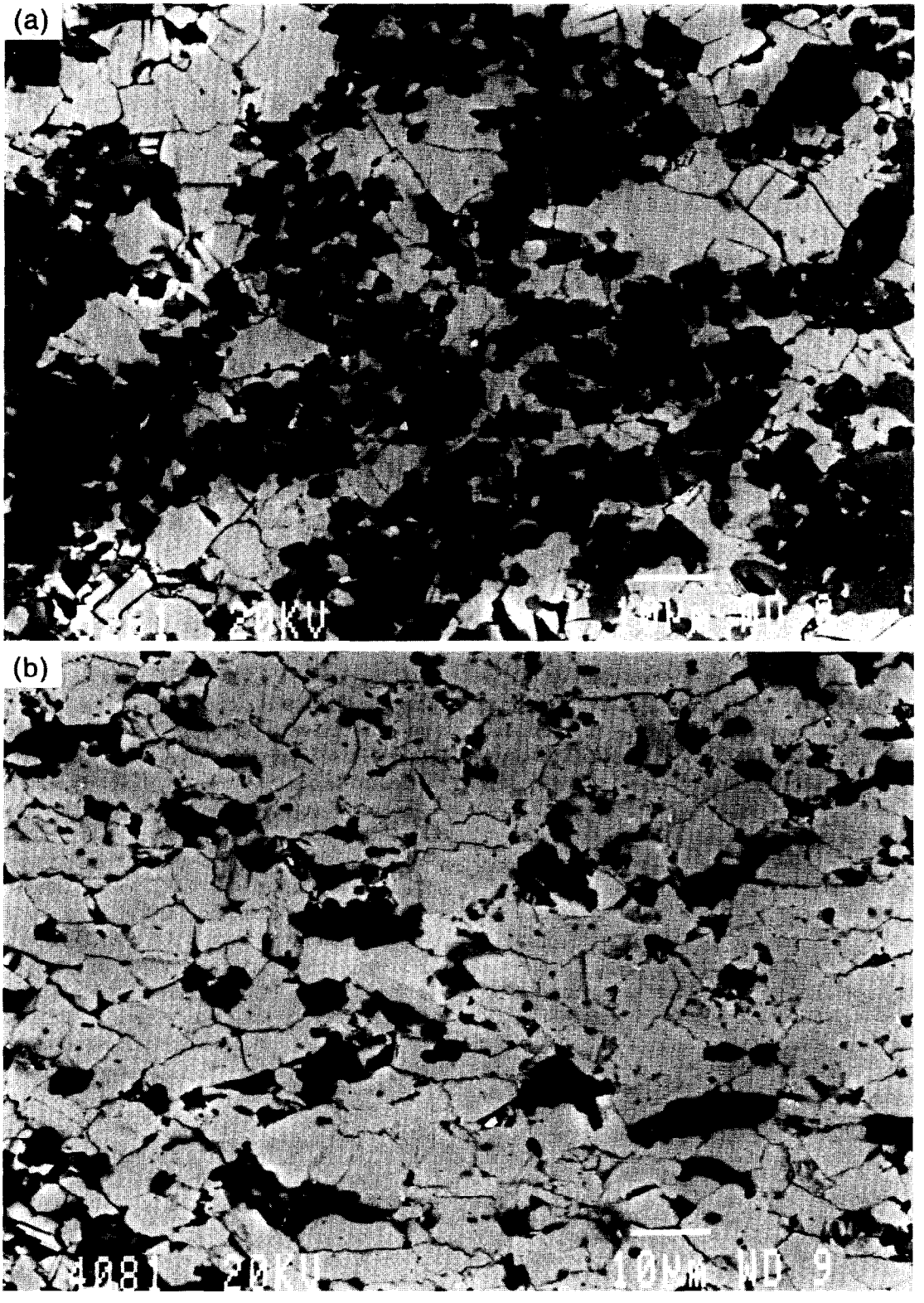

Fig. 2. SEM backscatter photomicrographs of Cc/An samples. White phase: anhydrite; grey phase: calcite; black: pores and holes generated during sample preparation. (a) 50/50 HIP#1; (b) 10/90 Cc/An.

In the pure anhydrite deformation is also by dominantly dislocation creep, but with some contribution of grain size sensitive diffusion mechanisms (Dell'Angelo and Olgaard, 1995). The characteristic microstructures are elongated grains, undulose extinction and relatively high dislocation densities. As the contribution of diffusion creep increases, there is a decrease in dislocation density, and the amount of grain flattening is reduced.

The synthetic calcite and anhydrite, used as end-

Table 2. Results from deformation experiments

Experiment no.	Cc:An	Stress (MPa)	Remarks
H1142	100 An	120	Strain: 20%*
H1258	100 An	120	Strain: 12%
H1259	100 An	130	Strain: 6%
H1145	100 Cc	98	Strain: 20%**
H1256	100 Cc	100	Strain: 6%
H1257	100 Cc	74	Strain: 12%
H1199	90:10	105	
H1215	70:30	78	
H1150	50:50#1	86	
H1198	50:50#2	65	
H1202	30:70	99	
H1203	10:90	170	

*Strain rate $= 2 \times 10^{-5}\,s^{-1}$; **strain rate $= 1 \times 10^{-4}\,s^{-1}$.

members for the mixtures, deform at similar stresses at the experimental conditions. At fast strain rates, anhydrite usually deforms at higher stresses, whereas at slower strain rates, the flow stress for calcite is higher (Fig. 1).

To investigate the development of texture with strain in the pure end-member phases, both pure calcite and pure anhydrite were deformed experimentally to strains of 6% and 12% at 500°C and a strain rate of $5 \times 10^{-5}\,s^{-1}$ (experiments H1256-59, Table 2) and their textures investigated. To complement these samples, textures were also analysed for pure anhydrite sample H1142, deformed at $2 \times 10^{-5}\,s^{-1}$ and for a pure calcite sample (H1145), deformed at $1 \times 10^{-4}\,s^{-1}$, both deformed to 20% strain but at stresses similar to those of the other pure samples (Table 2). In the two-phase rocks, both calcite and anhydrite preferred orientations were measured for the samples with varying volume proportions of calcite and anhydrite deformed at 500°C and a strain rate of $5 \times 10^{-5}\,s^{-1}$ (90:10 Cc:An: H1199; 70:30 Cc:An: H1215; 30:70 Cc:An: H1202; 10:90 Cc:An: H1203; 50:50 HIP#1: H1150; 50:50 HIP#2 H1198). All of the two-phase aggregates for texture goniometry were deformed to 20% shortening strain.

PREFERRED ORIENTATION DETERMINATION

The crystallographic preferred orientations of both the calcite and the anhydrite were measured by X-ray texture goniometry. The data were collected using a Scintag XDS 2000 texture goniometer with a solid-state detector. The measurements were carried out in transmission mode on thin sections, 50 μm thick, cut parallel to the compression axis.

The textures of materials deformed in uniaxial compression are rotationally symmetric about the compression axis, and consequently the preferred orientation of a given crystal plane can be measured by a profile scan taken (here at 5° intervals) from the parallel to the compression axis to an angle of 90° to it.

The pure end-member calcite and anhydrite samples were measured with a 1-mm collimator, 3-mm scatter slit and 2-mm receiving slit. Eight diffraction peaks were measured for calcite and 11 for anhydrite. For the pure calcite samples, the eight diffraction peaks measured are: 012 (f), 104 (r), 006 (c), 110 (a), 113, 202 (h), 024/018 (e) and 116 (Fig. 3). For the calcite component in the two-phase rocks, the diffraction peaks for 104 (r), 110 (a), 113 and 024/018 (e) were resolved (Fig. 3). For the pure anhydrite samples, the peaks measured are 111, 002/020, 200, 210, 022, 202/220, 212, 113, 301, 230 and 232 (Fig. 3). Diffraction peaks for 002 and 020 and for 202 and 220 overlap, with varying contributions of each slip plane to the diffraction intensity (Table 3). For the anhydrite in the two-phase rocks, diffraction peaks for 002/020, 210, 202/220, 212 and 301 were resolved (Fig. 3). The values of diffraction angles and background counting positions are shown in Table 4. The low symmetries of calcite (trigonal) and anhydrite (orthorhombic) result in a large number of diffraction peaks. In order to resolve these peaks in the two-phase rocks, a fine collimator (0.5 mm), scatter slit (2 mm) and receiving slit (1 mm) were used. This choice of slits allowed five anhydrite peaks and three calcite peaks to be measured. The fine slits and the fact that the volume fraction of each mineral was less than 1 resulted in very low count rates at the receiver which was compensated for by long counting times (Table 5). Two closely spaced peaks of calcite (024 and 018) were measured together, using the conventional 1-mm collimator, 3-mm scatter slit and 2-mm receiving slit. The radiation used was Cu K_α with the K_β peak removed by filtering after detection. This technique allows the measurement of the extremely weak signals resulting from the mixtures.

The pole figure scans were combined to give an inverse pole figure, using the harmonic method implementation

Table 3. Diffraction plane orientations for the pure end-members

No.	2θ	Plane	Polar angle	Azimuth	Intensity
(a) Calcite					
1	23.02	012	63.1	60.0	1.0
2	29.40	104	44.6	0.0	1.0
3	31.40	006	0.0	0.0	1.0
4	35.96	110	90.0	30.0	1.0
5	39.40	113	66.3	30.0	1.0
6	43.14	202	75.8	0.0	1.0
7	47.49	024	63.1	60.0	0.15
		018	26.3	60.0	0.85
8	48.41	116	48.8	30.0	1.0
(b) Anhydrite					
1	22.962	111	56.4	41.8	1.0
2	25.443	002	0.0	0.0	0.55
		020	90.0	90.0	0.45
3	28.606	200	90.0	0.0	1.0
4	31.373	210	90.0	24.1	1.0
5	36.297	022	45.0	90.0	1.0
6	38.645	202	48.3	0.0	0.91
		220	90.0	41.8	0.09
7	40.836	212	50.9	24.1	1.0
8	43.341	113	72.7	69.5	1.0
9	45.474	301	73.5	0.0	1.0
10	48.679	230	90.0	53.2	1.0
11	55.733	232	61.9	53.2	1.0

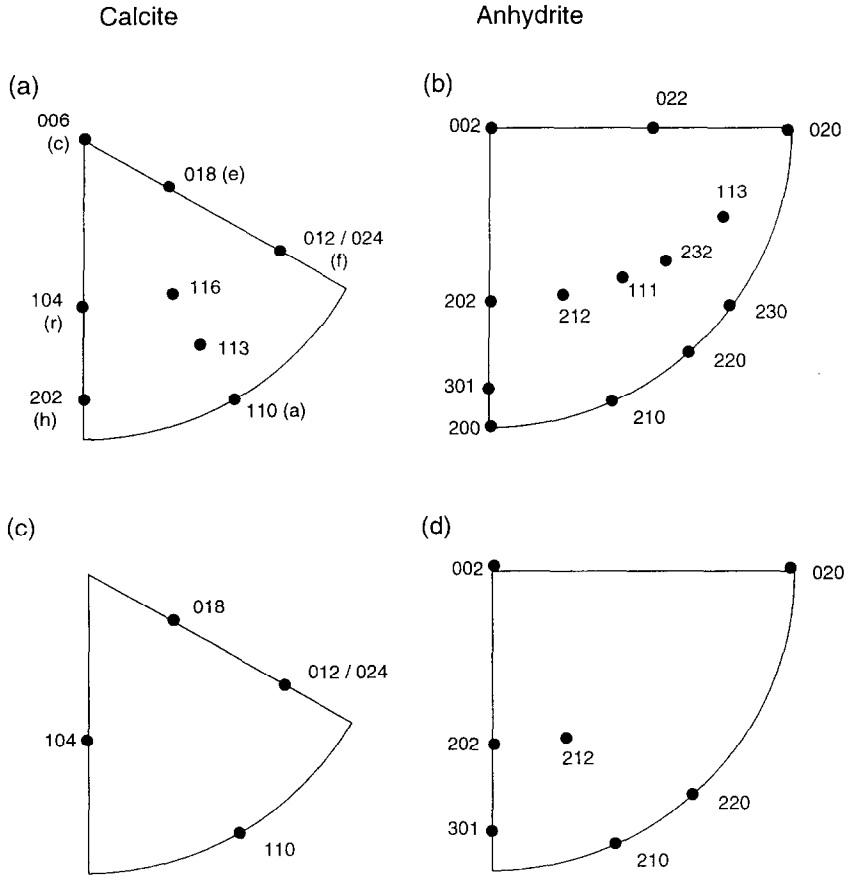

Fig. 3. Schematic inverse pole figures, indicating the planes measured in (a) pure calcite, (b) pure anhydrite, (c) calcite in the two-phase rocks and (d) anhydrite in the two-phase rocks

Table 4. Values of diffraction angles and background counting positions in the pure end-member phases

Plane	2θ	$2\theta_l$	$2\theta_r$	Scan rate ($^\circ s^{-1}$)
(a) Calcite				
012	23.02	20	25	30
104	29.40	27	33	60
006	31.40	27	33	10
110	35.96	34	38	30
113	39.40	38	41	30
202	43.14	41	45	30
024	47.49	45	50.5	30
116	48.41	45	50.5	30
(b) Anhydrite				
111	22.962	20	24	15
002	5.443	24	27.4	60
200	28.606	27.4	29.8	10
210	31.373	29.4	33.65	30
022	36.297	33.65	37.4	30
202	38.645	37.4	39.7	30
212	40.836	39.7	42.4	30
113	43.341	42.4	44.3	10
301	45.474	44.35	46	10
230	48.679	47.6	50.8	30
232	55.733	54.5	57	30

Table 5. Values of diffraction angles and background counting positions in the two-phase rocks

Plane	2θ	$2\theta_l$	$2\theta_r$	Counting time (s)
(a) Calcite				
104	29.40	28	30.5	40
110	35.96	35	37	60
113	39.4	37.5	40	30
(b) Anhydrite				
002	25.44	24	27	40
210	31.373	30.5	33	60
202	38.64	37.5	40	60
212	40.84	40	42	60
310	45.4	44.2	46	160

of Casey (1981). Table 5 shows the orientation of the diffraction peaks in relation to the crystal coordinate system and, in the case of overlapping peaks (002/020 and 202/220 in anhydrite), the relative intensity contributions of each component. The diffraction normals are shown in equal area stereographic projection for anhydrite and calcite in Fig. 3. The upper figure shows the full set of diffraction peaks used for the pure materials and the lower the reduced set used for the mixtures. The reduced set allowed a harmonic expansion of the inverse pole figure up to degree eight to be calculated. It can be seen from the inverse pole figures of the pure materials (Figs 4 and 5) and from those of the calcite and anhydrite in the two-phase rocks (Figs 5–7) that the complexity of the distributions can be adequately represented with this

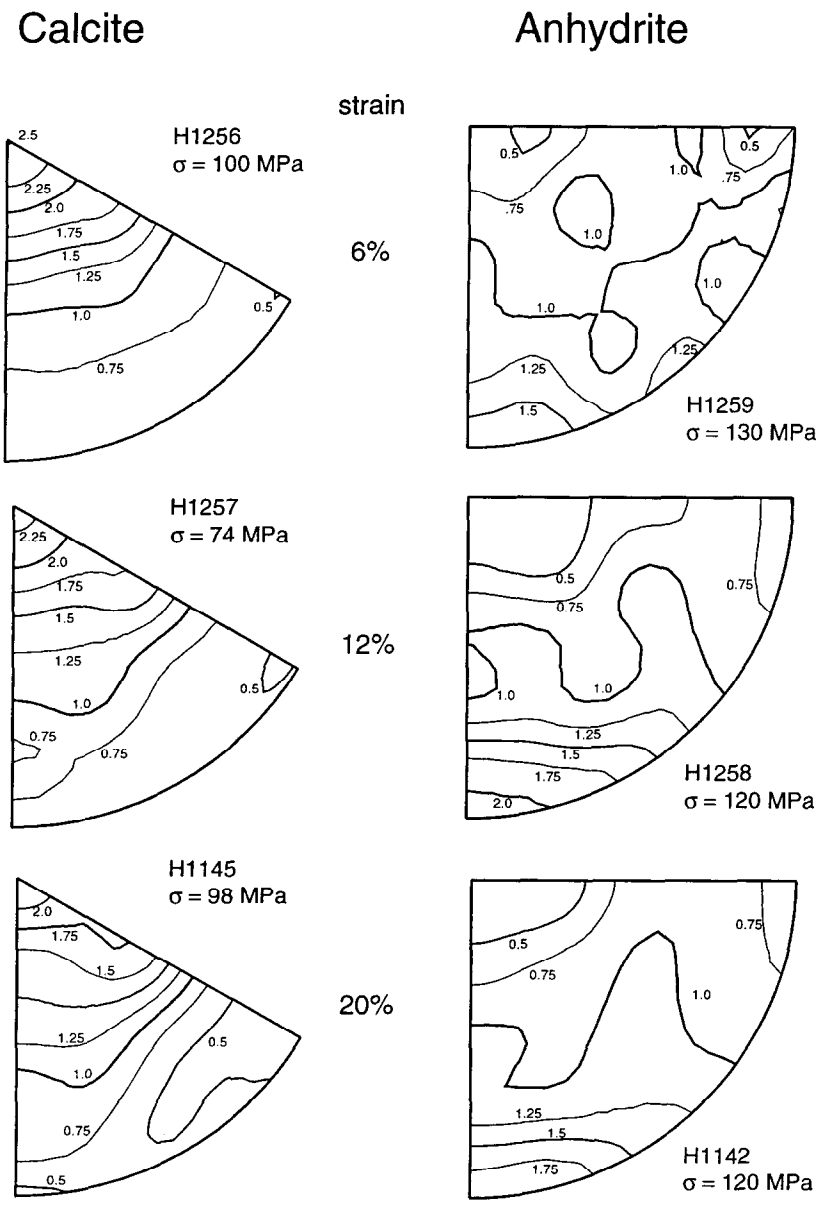

Fig. 4. Inverse pole figures of pure calcite and pure anhydrite deformed to various strains. Note different stresses. A contour of 1.00 represents a uniform distribution.

order of expansion. Figures 8–11 show the input data pole figures and pole figures regenerated from the harmonic expansion of the inverse pole figure for calcite and anhydrite from the 90/10 Cc/An 10/90 Cc/An mixtures. There is good agreement between measured and regenerated pole figures, indicating that the input pole figures are consistent. Contours of 1.00 represent a uniform distribution in the inverse pole figures and correspond to a probability of 1 in the pole figure profiles.

As the intensity of the preferred orientation of a deformed aggregate is investigated in terms of strain, some means of quantifying the texture is needed. A good measure of this intensity is the texture index, which is a quantitative expression of how far the distribution differs from uniformity. The texture index can be calculated for individual pole figures, as for this study, or for the inverse pole figure. The texture index, I, is defined by the equation

$$I = \int_0^{\frac{\pi}{2}} (\rho(\phi) - 1)^2 \sin\phi \, d\phi, \qquad (1)$$

where $\rho(\phi)$ is the probability, measured in multiples of a uniform distribution of the chosen crystallographic: direction, at an angle of ϕ from the compression direction. Uniformity is equal to 1 in pole figure profiles, whereas maxima are > 1, and depleted areas are < 1. The term 'texture index' as used in this publication is always the deviation from unity. The uncertainty in the texture index from the X-ray measurement assessed by the X-ray counting statistics is $< 5\%$.

Textures in calcite and anhydrite

Textures for the end-member phases of this study, i.e.

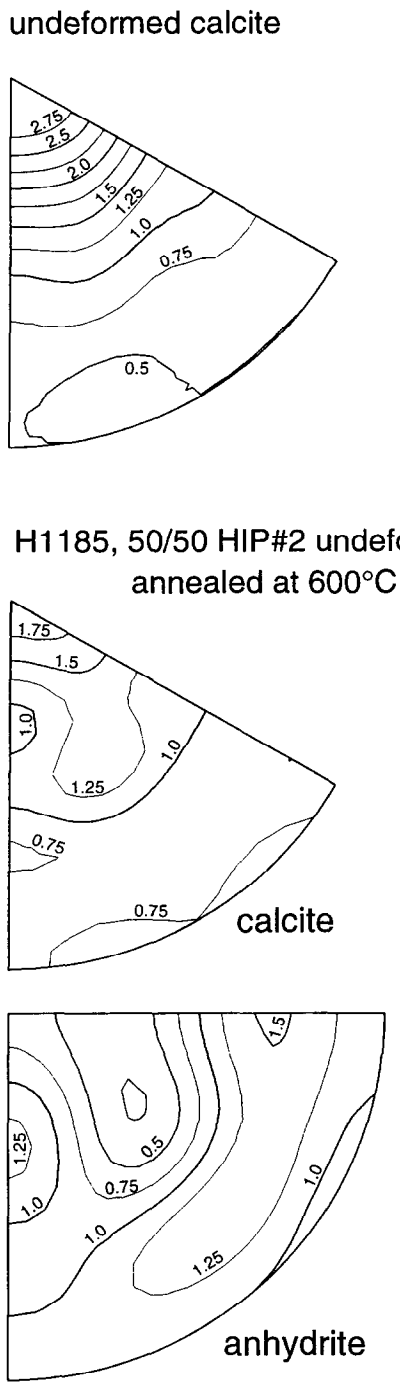

Fig. 5. Inverse pole figures for the undeformed calcite sample and for calcite and anhydrite in the undeformed 50/50 HIP#2 sample. A contour of 1.00 represents a uniform distribution.

calcite and anhydrite, have been investigated in previous studies, and the results of these studies are summarized here with reference to their representation on inverse pole figures (Fig. 3). The coordinate frame used to specify calcite orientations is the trigonal (hexagonal) cell.

The most commonly observed preferred orientations in calcite may be accounted for by slip on r and f, accompanied by twinning on e (Wenk, 1985). The maximum shortening strain that can be accommodated by e twinning is 29% in calcite single crystals and probably does not exceed 15% in polycrystalline aggregates (Wenk, 1985). Further deformation has to be accommodated by slip. At low temperatures, twinning on e leads to a concentration of the compression direction close to c, whereas slip on r causes a shoulder towards e (Wenk *et al.*, 1973). At higher temperatures, e twinning is reduced, and the contributions of r and f slip become more pronounced. The characteristic textures are a strong maximum at e and a ridge from a to h, and minima at f and r (Casey *et al.*, 1978). At conditions of low stress at high temperatures, only a weak preferred orientation was observed by Schmid *et al.* (1977) in fine-grained Solnhofen limestone, which is attributed to the dominance of superplastic flow, involving little intracrystalline plasticity.

In anhydrite, the operative slip systems are on (001) in direction of [010], and on (012) in directions $[\bar{1}\bar{2}1]$ and $[1\bar{2}1]$. Both slip systems operate at all temperatures (Mainprice *et al.*, 1993, and references therein), whereas twinning on {101} parallel to the edge of (101) and (010) is only active at temperatures >300°C at experimental strain rates. The maximum shortening strain accommodated by twinning is about 20% (Müller *et al.*, 1981). At low temperatures, the anhydrite texture is characterized by a maximum at (100) in the inverse pole figure, which is attributed to twinning. With increasing strain, the maximum broadens, developing a strong shoulder towards (210) and towards (301), while the region at (010) is depleted. This depletion has been interpreted as being due to rotation caused by glide on the two slip systems (Müller *et al.*, 1981). At higher temperatures, an additional maximum at (101) is developed (Dell'Angelo and Olgaard, 1995), which is also attributed to the operation of one or both of the slip systems. In the diffusion creep regime, a random CPO is found in synthetic anhydrites (Dell'Angelo and Olgaard, 1995).

RESULTS

Mechanical data

Results of the deformation experiments performed on the pure calcite and anhydrite aggregates and on the two-phase rocks are listed in Table 2 and plotted on Fig. 12. The stress values for the pure end-member materials calcite and anhydrite are similar, anhydrite being slightly stronger than the pure calcite. One of the pure calcite samples (H1257) was deformed at a lower stress than the two other calcites; no experimental reason could be found to explain this deviation from the stresses observed for the other samples.

The mixture with 90:10 Cc:An (H1199) was deformed at a stress similar to that of the pure calcite. For the sample with the mixture of 10:90 Cc:An (H1203), the stress was somewhat higher than for pure anhydrite. The 30:70 Cc:An (H1202), the 70:30 Cc:An (H1215) and the 50:50 HIP#1 (H1150) and HIP#2 (H1198) deformed at

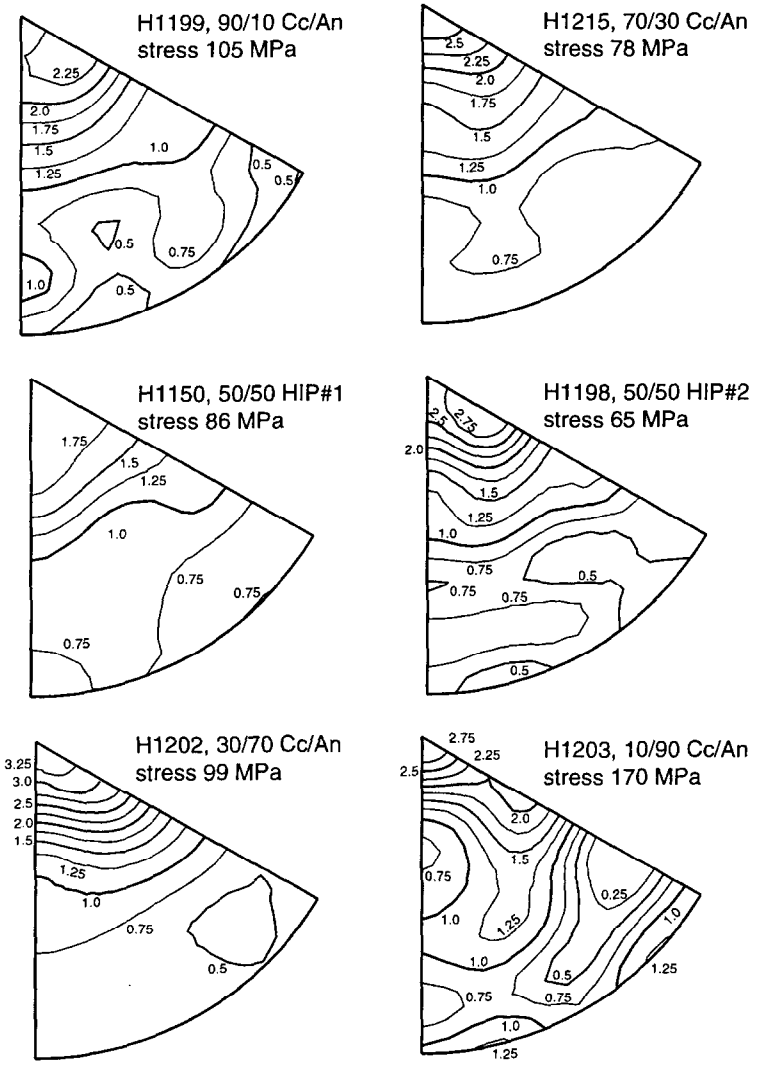

Fig. 6. Inverse pole figures for calcite in two-phase rocks with varying compositions deformed to 20% strain at 500°C and 5×10^{-5} s^{-1}. A contour of 1.00 represents a uniform distribution.

lower stresses than either end-member, stress values for the 50:50 HIP#2 (H1198) being lower than those for any other mixture.

Microstructures

It proved to be easiest to separate the phases for microstructural investigation using Scanning Electron Microscopy (SEM) backscatter images. The linear intercept method was used to determine the grain sizes on photomicrographs taken from SEM back scatter images, using 15×20, 20×30 and 30×40 line grids with lines parallel and perpendicular to the shortening direction on a transparency placed over the photomicrograph. Grain sizes given are the mean linear intercepts without any correction factor. The point counting method (e.g. Underwood, 1970) was used to determine the area proportion of the phases on each photomicrograph. Results of the grain counts are listed in Table 1.

Following the standard procedure (e.g. Schmid *et al.*, 1977) to determine the amount of grain flattening, grain aspect ratios, R, as given in Table 1, were calculated by equation (2) from the grain sizes (d) measured parallel and perpendicular to the shortening direction, assuming constant volume and initially spherical grain shapes:

$$R = \left(\frac{d_{\text{parallel}}}{d_{\text{perpendicular}}}\right)^{2/3} - 1. \quad (2)$$

In all the aggregates, calcite and anhydrite have approximately the same R values, except for the 90:10 Cc:An mixture (H1199), where the calcite is significantly more flattened (Table 1). Comparison with the undeformed samples (H1185, 50:50 and 90:10 Cc:An) shows that there is some initial flattening in the starting materials.

Preferred orientations

The inverse pole figures for the pure calcite aggregates show a strong maximum at c, with a shoulder towards e

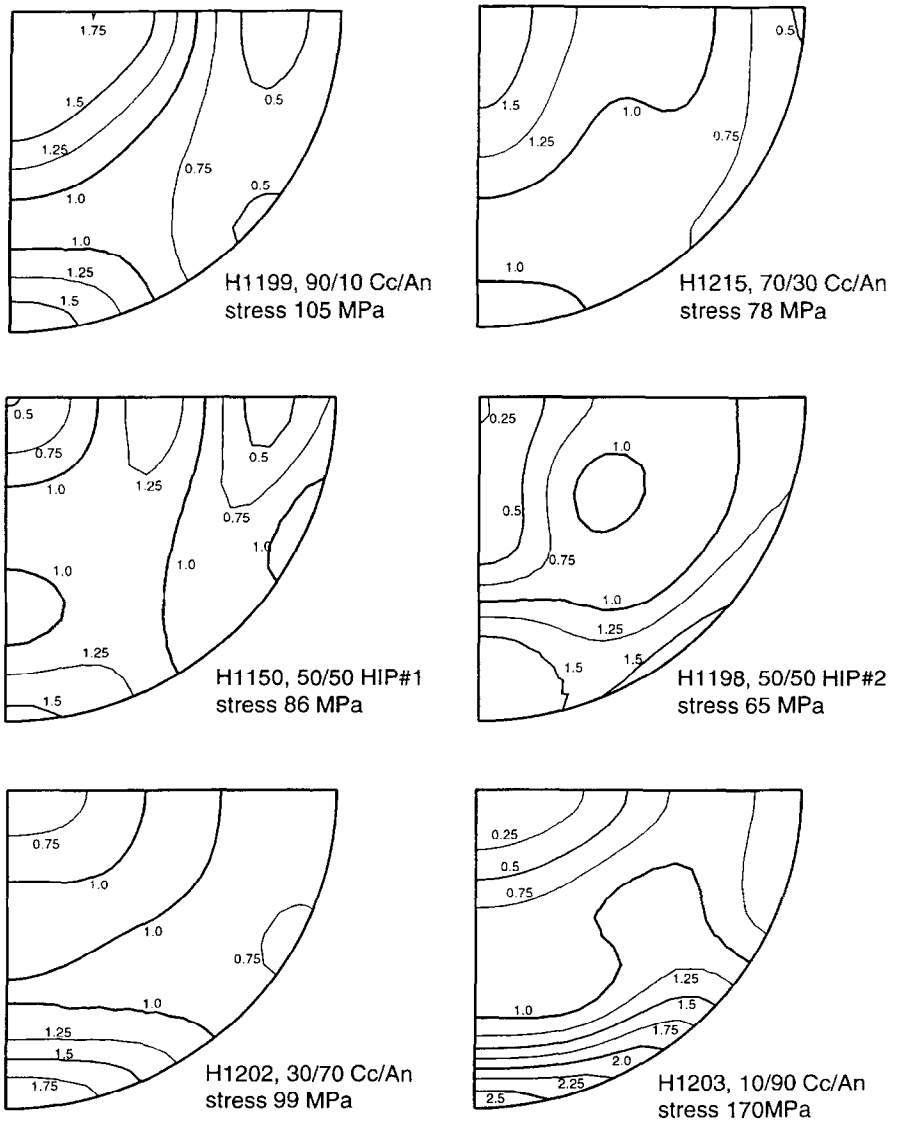

Fig. 7. Inverse pole figures for anhydrite in two-phase rocks with varying compositions deformed to 20% strain at 500°C and 5×10^{-5} s^{-1} A contour of 1.00 represents a uniform distribution.

(Fig. 4), suggesting that twinning and slip on r were operative. A maximum extending from a to h is commonly observed for deformed calcite aggregates at these conditions (e.g. Casey *et al.*, 1978), but that maximum is not developed for any of the pure calcite samples in this study. The undeformed calcite also has a strong maximum at c (Fig. 5). In the deformed calcite samples, the intensity of the maximum at c is slightly reduced with strain and develops a shoulder towards e. The strongest maximum at e was derived for the sample with the highest strain (H1145).

In the pure anhydrite samples, the inverse pole figures show patterns previously reported for experimentally deformed synthetic (Dell'Angelo and Olgaard, 1995) and natural anhydrites (Müller *et al.*, 1981). In the samples measured for this study (Fig. 4), a maximum is developed at (200) with a shoulder towards (210). A weak maximum is also developed at (202) in one anhydrite sample. This texture pattern is in agreement with that observed by Dell'Angelo and Olgaard (1995) for their deformation regime 1b. This regime is dominated by recovery mechanisms such as dislocation climb, which are identified by subgrain walls and recrystallized grains. The maximum at (200) and the shoulder towards (210) have been interpreted to be caused by twinning (Müller *et al.*, 1981). In the undeformed samples, the CPO is virtually random (Dell'Angelo and Olgaard, 1995).

The texture indices were calculated from the pole figure profiles (Fig. 7) for e in pure calcite and for r and e of the calcite components in the mixtures (Table 6). For anhydrite, the index was calculated for the maximum at (210) in both the pure materials and the two-phase rocks. In the pure calcite samples, the sample with the highest strain (H1145) had the highest texture index, whereas the sample with intermediate strain (H1257) had the lowest value. The indices reflect the qualitative observation from the inverse pole figures. In pure anhydrite, the texture index is highest for the sample with intermediate strain

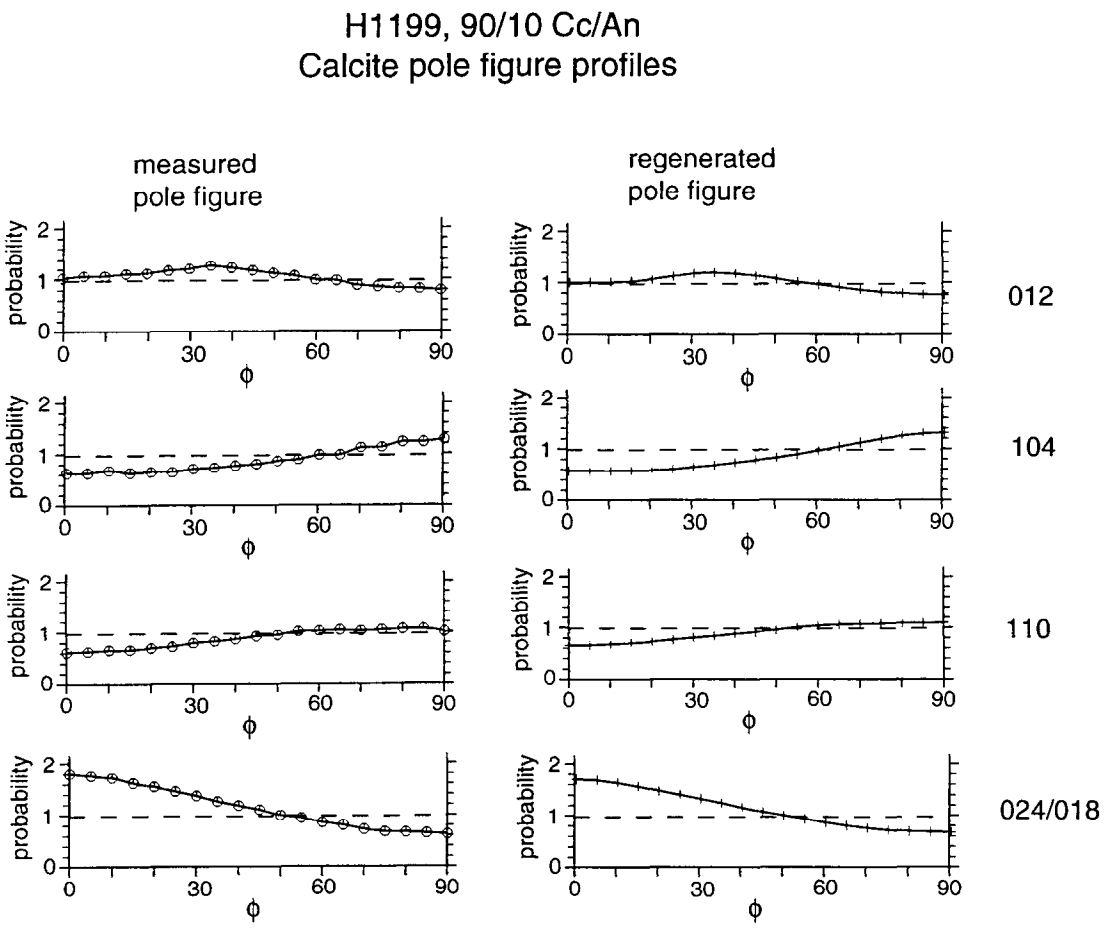

Fig. 8. Measured and recalculated pole figure profiles for calcite in the 90/10 Cc/An. The compression axis is at $\phi = 0°$.

(H1158) and lowest for the sample with the lowest strain (H1159).

The calcite CPO in the 90:10 Cc:An sample (Fig. 6) is qualitatively similar both to that described for the pure calcite samples and to that described for other calcite rocks which had deformed by intracrystalline mechanisms other than twinning, i.e. there is a maximum at e and a weak maximum at h. However, the CPO is more strongly developed than in the pure synthetic calcite aggregate (Fig. 4). For all the other mixtures, the pattern is slightly different, with a strong maximum at c and for some samples at e, and almost no development of the ridge from a to h, suggesting that twinning was the main CPO forming intracrystalline deformation mechanism in those samples. In the 10:90 Cc:An sample (Fig. 6), the calcite texture does not follow the general pattern observed for the pure calcite samples. Maxima are developed at c and e, and a weak maximum is developed between r and c, whereas minima are developed at f and h.

The texture indices for the calcite component in the various mixtures show a more systematic correlation with stress than with composition (Fig. 12). The index calculated for (018) is relatively low for the 10:90 Cc:An sample (Table 6), reaches a maximum for the 50:50 HIP#2 sample and then decreases with increasing calcite content. It seems to be inversely correlated with the sample stress. An exception is the 50:50 HIP#1 sample, which deformed at a relatively low stress and for which a relatively low calcite (018) texture index was calculated. For the texture index of (104), the inverse correlation is less pronounced. The value is lowest for the 10:90 Cc:An sample, a peak value is attained for the 30:70 Cc:An, and then the value decreases with increasing calcite content to a minimum at 50:50 Cc:An HIP#1, before increasing again at higher calcite contents (Table 6).

The texture patterns for the anhydrite component observed in the two-phase rocks are similar, but not identical, to those previously described for pure anhydrite samples. In all the samples, a maximum is developed around (200) and (210), whereas the weak maximum at (202) described for some pure anhydrite samples (Dell'Angelo and Olgaard, 1995) does not develop in any of the two-phase rocks (Fig. 7). The maximum at (200) with a shoulder towards (210) suggests that twinning is active in all the samples, particularly in those with $\geq$50 vol% anhydrite and in the 90:10 Cc:An, whereas other slip systems, characterized by the development of a maximum at (202), which are sometimes operative in pure anhydrite deformed at similar conditions (Dell'Angelo and Olgaard, 1995; this study), do not seem to be operative in the anhydrite component of the

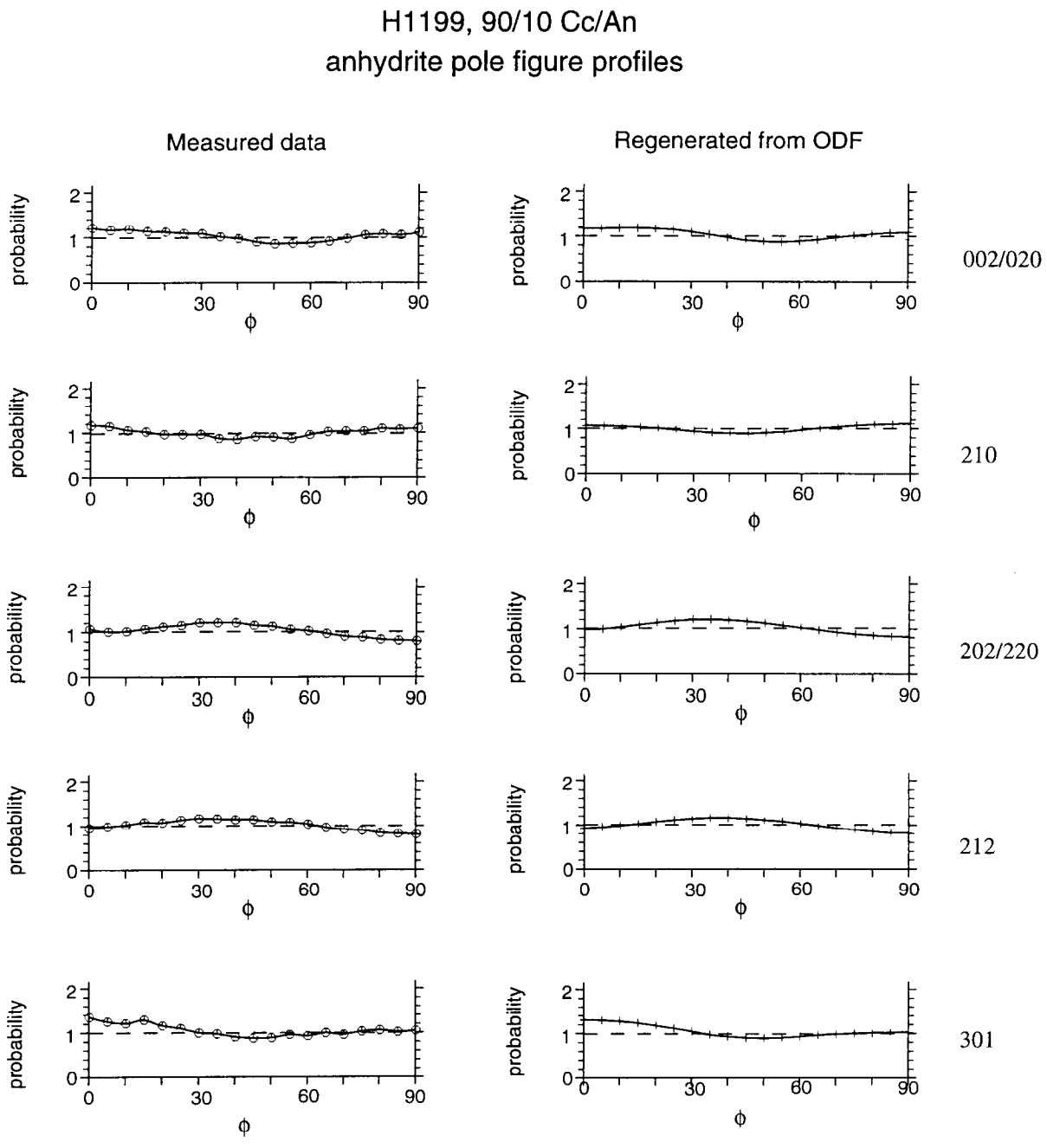

Fig. 9. Measured and recalculated pole figure profiles for anhydrite in the 90/10 Cc/An. The compression axis is at $\phi = 0°$.

two-phase rocks. In the samples with only 10% and 30% anhydrite, a weak maximum at (002) and a corresponding minimum at (020) are observed in the inverse pole figures (Fig. 7). The pole figure profiles for the overlapping (002) and (020) peaks (Fig. 9), from which the texture indices and the inverse pole figures are calculated, show no deviation from uniformity for (002/020), suggesting that the maximum and minimum present in the inverse pole figure are computational artifacts. In general, the intensity of the texture, as well as the texture index for anhydrite (210), decrease with decreasing anhydrite content (Fig. 7 and Table 6). In Fig. 12(c), the texture index of (210) for the anhydrite component is compared to the composition and the stress of the samples. The texture index seems to correlate with composition and with the stress. An exception is the 50:50 HIP#2 sample (H1198), for which the texture index is relatively high, but the stress is lower than for any other sample.

DISCUSSION

Deformation mechanisms

The deformation regimes for the pure end-members of the two-phase rocks at the experimental conditions are known from previous studies (Olgaard and Dell'Angelo,

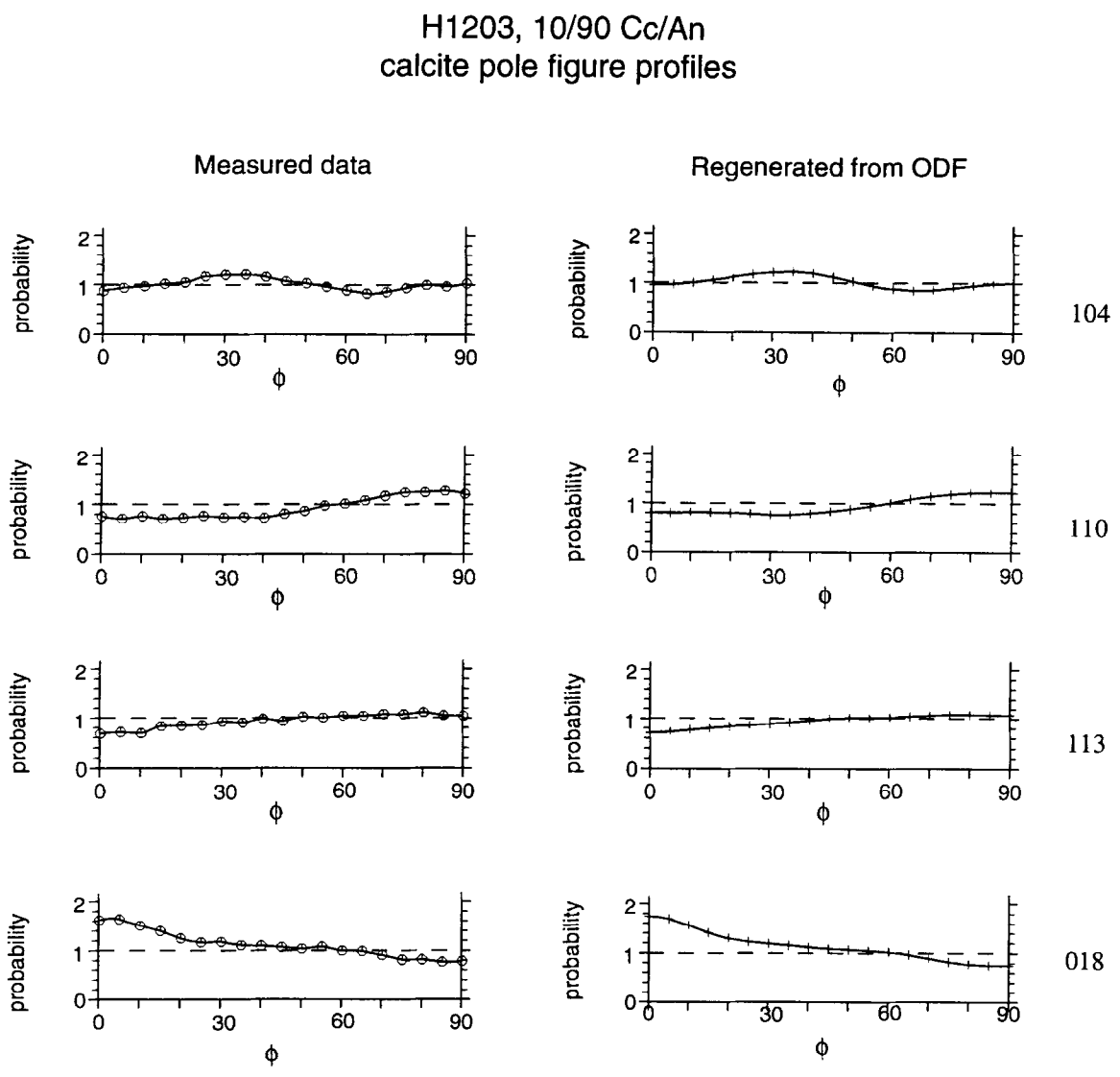

Fig. 10. Measured and recalculated pole figure profiles for calcite in the 10/90 Cc/An. The compression axis is at $\phi = 0°$.

1993; Dell'Angelo and Olgaard, 1995). Pure calcite is deformed by dominant dislocation creep mechanisms, whereas deformation of the pure anhydrite is in the transition region from dislocation to diffusion creep dominated flow (Fig. 1). Since diffusion creep is much more strongly grain size-sensitive than dislocation creep, the smaller grain sizes of the anhydrite component in the two-phase rocks, compared to that in the pure anhydrite samples, should have a noticeable effect on the contribution of diffusion creep and on the flow stress of the samples, depending on the volume proportion of the phases. Any variations in the relative significance of dislocation creep and diffusion creep also will affect the observed evolution of the CPO.

The relative contribution of dislocation creep and diffusion creep should be at least approximately indicated by the degree of grain flattening undergone by each phase (Table 1), calculated from the grain sizes parallel and perpendicular to the shortening direction (equation (2)). However, because of the initial shape preferred orientation measured for the two undeformed samples (H1185, Table 1), grain flattening does not necessarily account for all of the sample strain in any of the samples. Thus, grain flattening data have to be interpreted with due caution. In the 10:90 Cc:An sample, both phases are more strongly flattened than in the other samples. This supports the view that dislocation creep contributed more strongly to the sample strain than in the other samples. In all the other samples, the amount of grain flattening seems to be similar, except for the 50:50 HIP#1 sample (H1150), for which the calculated flattening was very small. In the 90:10 Cc:An sample, calcite grains are also strongly flattened.

Texture analysis

The data obtained for pure calcite and pure anhydrite, deformed at similar experimental conditions, show that a simple correlation of texture development with strain is not always possible. The intensities of the textures (and

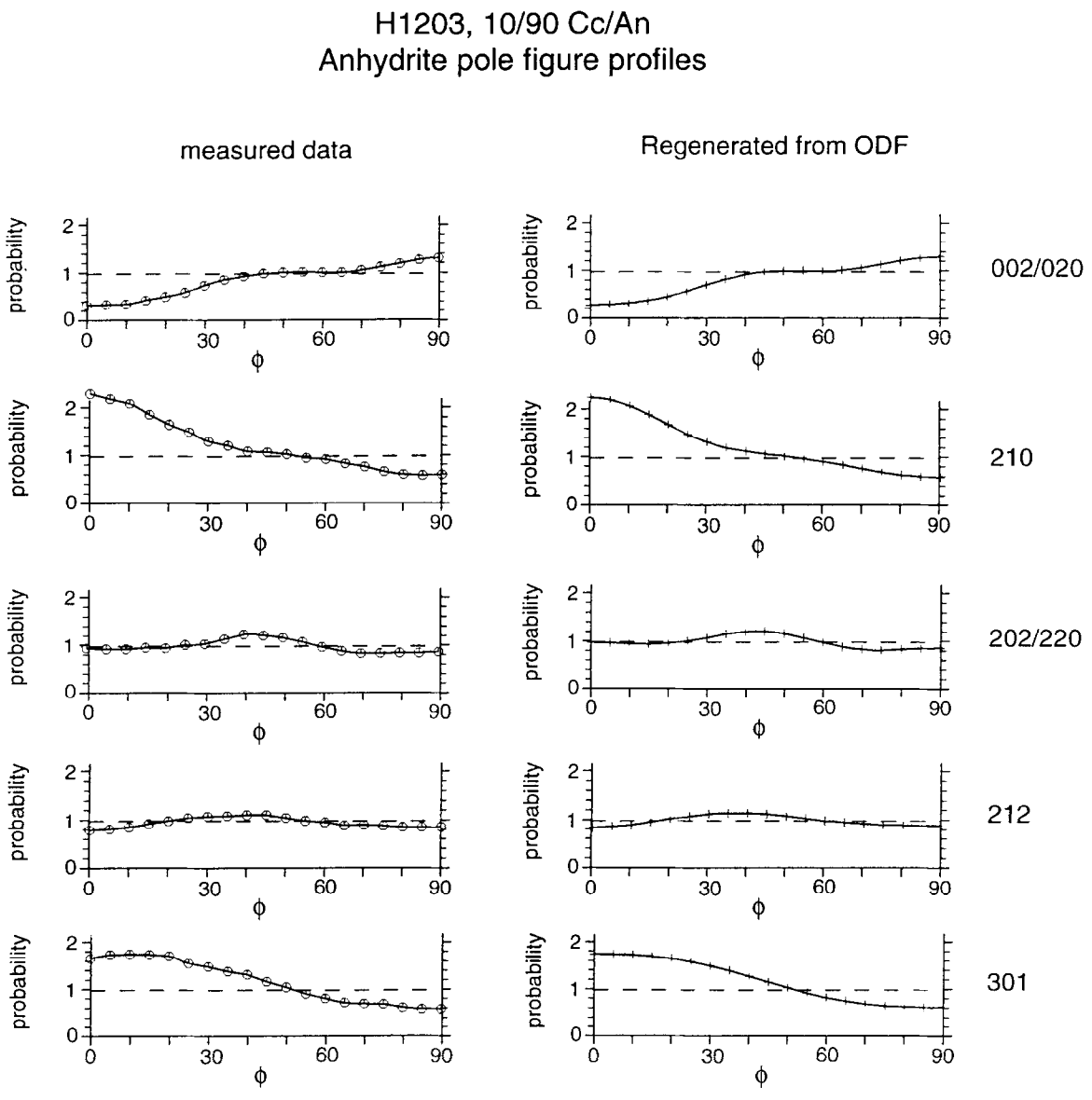

Fig. 11. Measured and recalculated pole figure profiles for anhydrite in the 10/90 Cc/An. The compression axis is at $\phi = 0°$.

the corresponding texture indices) in the pure calcite and the pure anhydrite samples do not depend clearly on strain, although strain was the only variable that was intentionally changed. In the pure calcite, although the texture index is largest for the sample deformed to 20% strain, the texture index is larger for the sample deformed to 6% strain than for the sample deformed to 12% strain. The lowest texture index coincides with the lowest stress measured for the experiments on pure calcite. The difference in the texture indices and thus the intensity of the texture development for pure calcite suggest that texture cannot be simply related to strain when the stresses are different.

In the pure anhydrite, the texture index for (210) in the sample deformed to 20% strain is lower than for the sample deformed to 12% strain, although the stresses for both samples were similar. This behaviour is not understood. A possible explanation for this observation arises from the experimental conditions, which are transitional between dislocation to diffusion dominated creep for pure anhydrite, suggesting that diffusion creep is more important in the finer grained part of the aggregates, and dislocation dominates deformation in the coarser grained parts. This interpretation is supported by similar observations made on anhydrite deformed at 400°C and 500°C (Dell'Angelo and Olgaard, 1995), where rheological data showed a large scatter at slow strain rates, which was interpreted to be due to varying contributions of diffusion creep because of slight differences in grain size. If correct, this interpretation would suggest that minor changes in the grain size distribution for a given mean grain size may have a major influence on the deformation mechanism (Bruhn, 1996) and therefore on the corresponding evolution of the microstructure and texture.

The texture patterns for pure calcite in this study (Fig. 4) are similar to, but not in complete agreement with

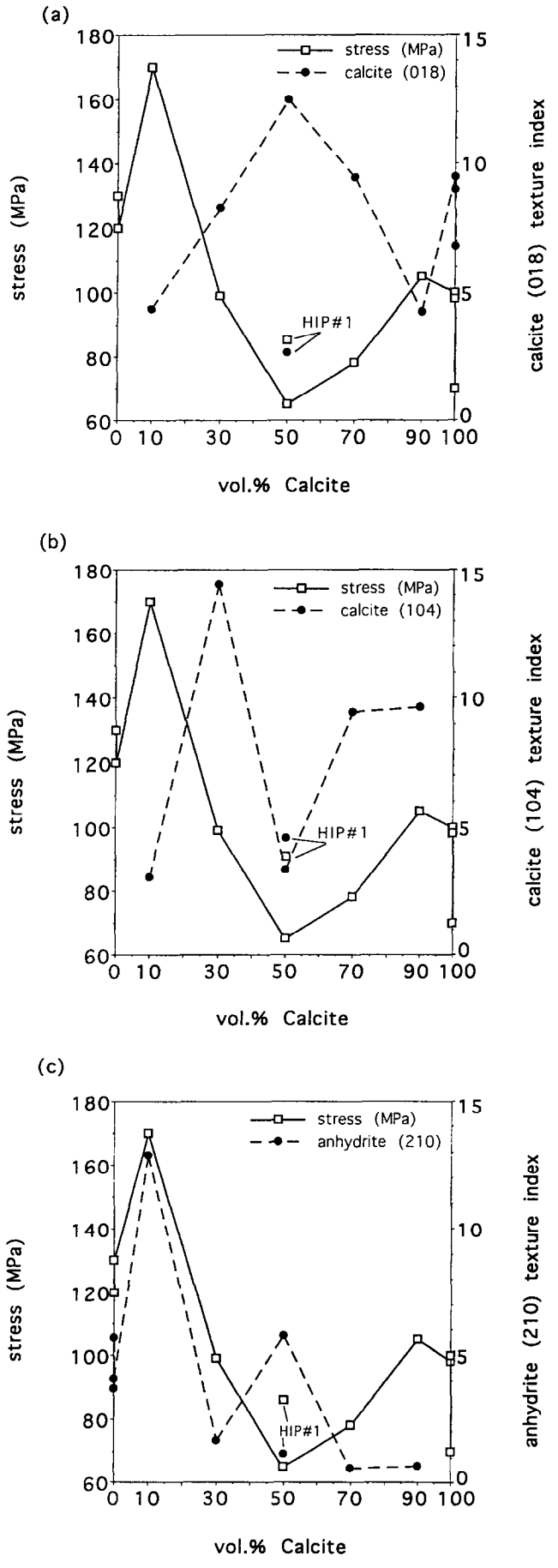

Table 6. Texture indices for three peaks: calcite 018 (e), calcite 104 (r), anhydrite 210, in pure calcite, pure anhydrite and two-phase rocks deformed at similar conditions

Sample no.	Mixture	Strain (%)	Stress (MPa)	Index		
				Cc 018	Cc 104	An 210
H1142*	100 An	20	120			1.0412
H1258		12	120			1.0573
H1259		6	130			1.0371
H1145**	100 Cc	20	98	1.0951		
H1256		6	100	1.0901		
H1257		12	70	1.0676		
H1199	90/10 Cc/An	20	105	1.0427	1.0965	1.0066
H1215	70/30 Cc/An	20	78	1.0946	1.0946	1.0059
H1202	30/70 Cc/An	20	99	1.0829	1.1443	1.0169
H1203	10/90 Cc/An	20	170	1.0439	1.0304	1.1292
H1150	50/50 Cc/An	20	86	1.0264	1.0455	1.0115
H1198	50/50 Cc/An	20	65	1.1250	1.0333	1.05611

*Strain rate = 2×10^{-5} s^{-1}; **strain rate = 1×10^{-4} s^{-1}.

previously published data for similar rocks (Casey *et al.*, 1978; Wenk *et al.*, 1981; Wenk, 1985; Rutter *et al.*, 1994). In those studies, maxima around c and e, as observed in our pure calcite samples, are commonly interpreted as being due to twinning on e. However, twinning has not been reported in previous studies on different fine-grained calcite rocks deformed at similar conditions (e.g. Schmid *et al.*, 1977; Walker *et al.*, 1990), nor was it widely observed in this study. Other features typically observed in inverse pole figures for fine-grained limestones deformed at intermediate stresses and temperatures are a distinct ridge between a and h, with weak maxima at e and c, and minima at f and r (e.g. Casey *et al.*, 1978; Rutter *et al.*, 1994). These features are usually interpreted as being due to higher temperature intracrystalline slip, but none of them was observed in the pure calcites or the calcite in the two-phase samples, except for the 90:10 Cc:An (Fig. 6) sample, where a weak maximum at h may represent the incipient ridge from a to h.

The maximum at c in the pure calcites is probably due to a preexisting fabric, as a relatively strong maximum at c is also found in an undeformed synthetic calcite sample (Fig. 5). Rutter *et al.* (1994) also observed a weak maximum at c in undeformed synthetic calcite samples, which were uniaxially cold-pressed and then hot isostatically pressed, but they also found that samples that were not uniaxially cold pressed prior to hot pressing had no initial CPO. Thus, the maximum observed in our samples may be explained by the sample preparation technique, as uniaxial cold-pressing was also used before the materials were hot isostatically pressed. The strains in our samples may not have been high enough to overprint this preexisting fabric, as the concentration of preferred orientations in the upper half of the inverse pole figure of

Fig. 12. Texture indices and stress plotted as a function of composition. The texture index units are deviation (× 100) from texture index 1 (randomness).

the undeformed calcite sample suggests an orientation of crystallographic axes with respect to the shortening axis that does not allow a later re-orientation to the lower half. Thus, the development of maxima in the lower half, like the a to h ridge, may have been inhibited.

The similarity of the textures in the two-phase rocks to those in the pure end-member materials obtained for this study suggests that essentially the same mechanisms operate in the mixtures as in the single phase aggregates. However, it is not obvious as to the cause of the intensity of the texture. The differences in the texture indices do not relate to bulk strain, which is similar for all the two-phase aggregates; therefore, the question remains as to whether they relate to the strain of the individual phases, similar to the quartz textures reported by Dell'Angelo and Tullis (1986). If the amount of grain flattening (Table 1) is at least a relative indicator of the amount of strain accommodated by one phase and if texture is related to strain only, then the anhydrite texture index should be lower for the 50:50 HIP#1 sample (H1150) than for the 70:30 Cc:An (H1215), because grains are less flattened in the 50:50 HIP#1 than in the 70:30 Cc:An. However, the anhydrite CPO is more strongly developed in the 50:50 HIP#1. However, the texture in the anhydrite component also may be related to the stress of the samples (Fig. 12) or rather the stress partitioned into the anhydrite, which, in turn, depends on the anhydrite grain size. The decreasing anhydrite grain size with decreasing anhydrite content results in an higher contribution of diffusion creep to the deformation of the anhydrite component. Thus, an increasing amount of bulk stress is accommodated by the calcite component, which deforms by mainly dislocation creep, as suggested by the textures and the grain flattening calculated from the photomicrographs (Table 1).

The relationship of the calcite texture indices to experimental parameters is more complex. The relatively low values of the texture indices for calcite in the 10:90 Cc:An sample (Table 6) for both (104) and (018), and the irregular texture pattern (Fig. 6) may be due to the high degree of dispersion of calcite in anhydrite (Fig. 2b) and resulting grain boundary constraints, since almost all of the calcite grains are completely surrounded by anhydrite, which may inhibit slip systems commonly observed in pure calcite. If the intensity of the (018) texture development depends inversely on the stress, as suggested by the correlation observed in Fig. 12, the relatively high values of the calcite texture indices for the 30:70, 50:50 HIP#2 and the 70:30 Cc:An samples may be due to a strain partitioning into the calcite component, if anhydrite is the stronger phase. However, the increased contribution of diffusion creep, which is also reflected by the weak anhydrite textures in these samples, to the deformation of the anhydrite component makes the anhydrite in the two-phase rocks weaker than the pure anhydrite and probably weaker than the calcite deforming by dislocation creep at the same experimental conditions. In this case, there should be a stress partitioning into the calcite component rather than a strain partitioning, which, in turn, may influence the relative significance of the different slip systems in calcite.

Since twinning in calcite is not observed in our samples, the higher concentration at e may be due to a reorientation of the compression direction from c towards e, which seems to be favoured at lower stresses. At higher stresses, the results of Casey *et al.* (1978) and Rutter *et al.* (1994) indicate that a maximum develops at c, and a preexisting maximum is retained at c. Consequently, the maximum at e does not develop as quickly. At lower stresses, the maximum develops at e, in which case, the texture index for (018) will be higher at lower stresses. However, these explanations do not account for the relatively low texture index for the (018) in the 50:50 HIP#1 sample. The texture index for (104) is a general indicator of the degree of CPO in calcite, but no direct correlation of texture index and any experimental variable was found. However, as pointed out above, the contribution of each slip system to the phase strain may vary considerably with phase stress.

CONCLUSIONS

The data obtained for this study indicate that texture may be highly variable in the transition region from one mechanism to another and that a simple correlation between strain and texture development has to take into account the effects of stress, grain size and possible changes in deformation mechanisms, even if the experimental or natural deformation conditions were constant.

In the anhydrite within the two-phase rocks there was a significant contribution of diffusion creep to the deformation. The relative contribution of diffusion creep increased with decreasing anhydrite content and the associated decrease in anhydrite grain size. This change in deformation mechanism in the two-phase rocks, compared to the (coarser grained) pure anhydrite aggregates, caused an overall reduction of the flow stress in the two-phase rocks. However, since only the anhydrite component was deformed at a lower stress, it is reasonable to assume some stress partitioning into the calcite component. Thus, the calcite stress in the two-phase rocks was probably higher than the bulk stress.

The texture development in calcite and anhydrite does not seem to be inhibited by the presence of the other phase. However, the associated texture development cannot simply be related to strain. From our experimental data and the textures derived for our samples, we conclude that both the textures of the pure materials and those of the two-phase rocks also critically depend on stress and grain size, which may influence the deformation mechanisms.

In the experimentally deformed single-phase and two-phase rocks of this study, the texture index seems to be related to the stress rather than to strain. In pure calcite, the texture index did not vary much between samples

deformed to 6% strain and 20% strain at the same stress, but it was clearly lower for a sample deformed to 12% strain at a lower stress. In the calcite component within the two-phase rocks, the texture index for (018) seems to be inversely related to the sample stress. However, no correlation is observed for the texture index of calcite (104). In the anhydrite component, the texture index decreases with stress and anhydrite content. This decrease in intensity of the anhydrite CPO and stress is attributed to the increasing contribution of diffusion creep with decreasing anhydrite grain size.

From the results of our investigation, we conclude that, unless the relative contributions of the various deformation mechanisms to the strain in the different phases are better constrained, texture analysis may not be used for a quantification of stress and strain partitioning between the phases in a polyphase material.

Acknowledgements—The results presented in this study are part of a Ph.D. thesis funded by the ETH Zürich. The authors wish to thank all the people who contributed to the improvement of this manuscript. My (D.B.) Ph.D. advisors Lisa Dell'Angelo and Dave Olgaard spent a lot of time preparing experiments, discussing the results and proof-reading the manuscript. Stimulating discussions with E. Rutter and K. Kunze helped with the interpretation of the textures. D. Grujic took the SEM photomicrographs. Very detailed and constructive reviews by S. Covey-Crump and B. Hacker helped to improve the manuscript significantly.

REFERENCES

Bouchez, J.-L. (1977) Plastic deformation of quartzites at low temperature in an area of natural strain gradient. *Tectonophysics* **39**, 25–50.

Bruhn, D. (1996). Rheology of fine-grained two-phase rocks with phases of similar strength — an experimental investigation. Unpublished PhD-thesis, ETH Zürich

Casey, M. (1981) Numerical analysis of X-ray texture data: an implementation in FORTRAN allowing triclinic or axial specimen symmetry and most crystal symmetries. *Tectonophysics* **78**, 51–64.

Casey, M., Rutter, E. H., Schmid, S. M., Siddans, A. W. B. and Whalley, J. S. (1978) Texture development in experimentally deformed calcite rocks. In *Textures of Materials, Proceedings of the 5th Industrial Conference on Textures of Materials*, eds. G. Gottstein and K. Lücke, Vol. 11, pp. 231–240, Aachen.

Casey, M., Dell'Angelo, L. N., Olgaard, D. L. and Siddiqi, G. (1991) Crystallographic preferred orientation development in experimentally deformed fine-grained anhydrite. *EOS Transactions of the American Geophysical Union* **72**, 459.

Dell'Angelo, L. N. and Olgaard, D. L. (1995) Experimental deformation of fine grained anhydrite: evidence for dislocation and diffusion creep. *Journal of Geophysical Research* **100**, 15425–15440.

Dell'Angelo, L. N. and Tullis, J. (1986) A comparison of quartz c-axis preferred orientations in experimentally deformed aplites and quartzites. *Journal of Structural Geology* **8**, 683–692.

Jordan, P. G. (1987) The deformational behaviour of bimineralic limestone–halite aggregates. *Tectonophysics* **135**, 185–197.

Kern, H. (1977) Preferred orientation of experimentally deformed limestone marble, quartzite and rock salt at different temperatures and stress. *Tectonophysics* **39**, 103–120.

Kronenberg, A. K. (1981) Quartz preferred orientations within a deformed pebble conglomerate from New Hampshire, USA. *Tectonophysics* **79**, T7–T15.

Law, R. D., Knipe, R. J. and Dayan, H. (1984) Strain path partitioning within thrust sheets: microstructural and petrofabric evidence from the Moine Thrust zone at Loch Eriboll, northwest Scotland. *Journal of Structural Geology* **6**, 477–497.

Lisle, R. J. (1985) The effect of composition and strain on quartz-fabric intensity in pebbles from a deformed conglomerate. *Geologische Rundschau* **74**, 657–663.

Lister, G. S. and Hobbs, B. E. (1980) The simulation of fabric development during plastic deformation and its application to quartzite: the influence of deformation history. *Journal of Structural Geology* **2**, 355–370.

Mainprice, D., Bouchez, J.-L., Casey, M. and Dervin, P. (1993) Quantitative texture analysis of naturally deformed anhydrite by neutron diffraction texture goniometry. *Journal of Structural Geology* **15**, 793–804.

Marjoribanks, R. W. (1976) The relation between microfabric and strain in a progressively deformed quartzite sequence from Central Australia. *Tectonophysics* **32**, 269–293.

Müller, W. H., Schmid, S. M. and Briegel, U. (1981) Deformation experiments on anhydrite rocks of different grain sizes: rheology and microfabric. *Tectonophysics* **78**, 527–543.

Olgaard, D. L. and Dell'Angelo, L. N. (1993) Another flow law for calcite rocks: reagent $CaCO_3$ powders densified by HIPing. *Terra abstracts, Abstract Supplement No. 1 to Terra Nova* **5**, 294.

Rutter, E. H., Casey, M. and Burlini, L. (1994) Preferred crystallographic orientation development during the plastic and superplastic flow of calcite rocks. *Journal of Structural Geology* **16**, 1431–1446.

Schmid, S. M., Boland, J. N. and Paterson, M. S. (1977) Superplastic flow in fine-grained limestone. *Tectonophysics* **43**, 257–291.

Spiers, C. J. (1979) Fabric development in calcite polycrystals deformed at 400°C. *Bulletin of Mineralogy* **102**, 282–289.

Starkey, J. and Cutforth, C. (1977) A demonstration of the interdependence of the degree of quartz preferred orientation and the quartz content of deformed rocks. *Canadian Journal of Earth Science* **15**, 841–847.

Tullis, J. and Wenk, H.-R. (1994) Effect of muscovite on the strength and lattice preferred orientations of experimentally deformed quartz aggregates. *Materials Science and Engineering* **A175**, 209–220.

Tullis, J., Christie, J. M. and Griggs, D. T. (1973) Microstructures and preferred orientations of experimentally deformed quartzites. *Bulletin of the Geological Society of America* **84**, 297–314.

Underwood, E. E. (1970) *Quantitative Stereology*. Addison-Wesley, Reading, MA.

Walker, A. N., Rutter, E. H. and Brodie, K. H. (1990) Experimental study of grain-size sensitive flow of synthetic, hot-pressed calcite rocks. In *Deformation Mechanisms, Rheology and Tectonics*, eds. R. J. Knipe and E. H. Rutter, Vol. 54, pp. 259–284. Special Publications of the Geological Society, London.

Wenk, H.-R. (1985) Carbonates. In *Preferred Orientations in Metals and Rocks: An Introduction to Modern Texture Analysis*, eds H.-R. Wenk, pp. 361–384. Academic Press, Orlando, FL.

Wenk, H.-R., Venkitasubramanyon, C. S. and Baker, D. W. (1973) Preferred orientation in experimentally deformed limestone. *Contributions in Mineralogy and Petrology* **38**, 81–114.

Wenk, H.-R., Kern, H. and Wagner, F. (1981) Texture development in experimentally deformed limestone. In *Deformation of Polycrystals: Mechanics and Models*, ed. Danish Risø National Laboratory, pp. 235–245. National Laboratory, Roskilde, Denmark.